Journal of Inorganic Biochemistry 191 (2019) 143–153

Contents lists available at ScienceDirect

Journal of Inorganic Biochemistry

journal homepage: www.elsevier.com/locate/jinorgbio

How copper ions and membrane environment influence the structure of the human and chicken tandem repeats domain?

Aleksandra Hecel[a,*], Daniela Valensin[b], Henryk Kozłowski[c]

[a] Faculty of Chemistry, University of Wroclaw, F. Joliot-Curie 14, 50383 Wroclaw, Poland
[b] Department of Biotechnology, Chemistry and Pharmacy, University of Siena, Via A. Moro 2, 53100 Siena, Italy
[c] Opole Medical School in Opole, Katowicka 68, 45060 Opole, Poland

ARTICLE INFO

Keywords:
Prion proteins
Copper ions
Histidine residues
Membrane mimicking environment
Micelles

ABSTRACT

Prion proteins (PrPs) from different species have the enormous ability to anchor copper ions. The N-terminal domain of human prion protein (hPrP) contains four tandem repeats of the –PHGGGWGQ– octapeptide sequence. This octarepeat domain can bind up to four Cu^{2+} ions. Similarly to hPrP, chicken prion protein (chPrP) is able to interact with Cu^{2+} through the tandem hexapeptide -HNPGYP- region (residues 53–94). In this work, we focused on the human octapeptide repeat (human $Octa_4$, $hPrP_{60–91}$) (Ac-PHGGGWGQPHGGGWGQPHGGGWGQPHGGGWGQ-NH_2) and chicken hexapeptide repeat (chicken $Hexa_4$, $chPrP_{54–77}$) (Ac-HNPGYPHNPGYPHNPGYPHNPGYP-NH_2) prion protein fragments. Due to the fact that PrP is a membrane-anchored glycoprotein and its unstructured and flexible N-terminal domain may interact with the lipid bilayer, our studies were carried out in presence of the surfactant sodium dodecyl sulfate (SDS) mimicking the membrane environment in vitro. The main objective of this work was to understand the effects of copper ion on the structural rearrangements of the human and chicken N-terminal repeat domain. The obtained results provide a fundamental first step in describing the thermodynamic (potentiometric titrations) and structural properties of Cu(II) binding (UV–Vis, NMR, CD spectroscopy) to both human $Octa_4$ and chicken $Hexa_4$ repeats in both a DMSO/water and SDS micelle environment. Interestingly, in SDS environment, both ligands indicate different copper coordination modes, which results of the conformational changes in micelle environment. Our results strongly support that copper binding mode strongly depends on the protein backbone structure. Moreover, we focused on previously obtained results for amyloidogenic human and chicken fragments in membrane mimicking environment.

1. Introduction

Prion proteins (PrPs) are associated with lethal neurodegenerative disorders grouped as transmissible spongiform encephalopathies (TSEs) [1–3]. The diseases are associated with a pathological and misfolded form of the normal cellular prion protein (PrP^C). This abnormal and toxic protein, known as scrapie (PrP^{Sc}), is rich in β-sheet structure, insoluble in water, protease-resistant and highly prone to aggregate [4]. Although the two prion protein (PrP) forms possess identical amino acid sequence [5–7], they exhibit different physical and chemical properties. In addition, it is well accepted that the structural rearrangement of PrP^{Sc} is a key process in the onset of the prion protein diseases.

Copper ions bind to human PrP^C in vivo [8]. Residues 60–91 in the unstructured N-terminal domain of PrP^C, consist of the replica of the octapeptide sequence -PHGGGWGQ-. This region is able to bind up to four Cu^{2+} ions cooperatively, forming a multi His complex. Copper binding to the octapeptide unit PHGGGWGQ at physiological pH involves the imidazole, two amide nitrogens donors, and Trp side-chain, which is brought close to Cu^{2+} through a metal ion bound water molecule [9–11]. Besides the four copper ions bound by the octapeptide domain, two additional and independent Cu^{2+} anchoring sites, encompassing H96 and H111 residues respectively are present [12–17]. The $hPrP_{91–127}$ region is called the amyloidogenic domain of human prion protein (hPrP) and seems to be essential for amyloid formation of prion disease [18,19].

The prion protein is not only specific for mammals, it is also seen in other species including avians, fish, reptiles and amphibians. The chicken prion protein (chPrP) shows around 30% identity with its mammalian analogue [20]. Similar to the human one, chPrP also contains a tandem region, including hexapeptide repeat units ($chPrP_{54–59}$

* Corresponding author.
E-mail address: aleksandra.hecel@chem.uni.wroc.pl (A. Hecel).

https://doi.org/10.1016/j.jinorgbio.2018.11.012
Received 18 August 2018; Received in revised form 19 November 2018; Accepted 21 November 2018
Available online 23 November 2018
0162-0134/

-HNPGYP-). Cu^{2+} coordination to the monomeric unit of chicken prion involves imidazole and deprotonated amide nitrogen donors [21,22]. chPrP is able to interact with Cu^{2+} also through the amyloidogenic region by two imidazole nitrogen atoms from histidine residues H110 and H124, respectively [23].

PrP binding to cell membrane occurs via its C-terminal glycosylphosphatidylinositol (GPI) anchor, such that it is reasonable to believe that the presence of lipid bilayers may have an influence on the Cu^{2+} binding ability of the prion protein octarepeat region. In addition, there are many evidences indicating that PrP^{Sc} toxicity is dependent on the ability of PrP to interact with lipid membranes [24–27]. Beyond PrP, other amyloidogenic proteins, like amyloid β and α-synuclein are able to bind and perturb micelles and lipid vesicles [28–30]. Finally, it has been recently reported that the membrane bound form of PrP is able to strongly interact with amyloid β oligomers [31].

First CD investigations on the conformational effect of lipid bilayers on human PrP^{C} showed some structuring effect on the N-terminal domain of the protein, with a parallel weak destabilization of the folded C-terminal globular domain [32]. Our previous studies showed that the amyloidogenic region of human hPrP91–127 and chicken chPrP105–140 prion protein undergoes random coil to α-helix transition in the presence of membrane mimicking environment (sodium dodecyl sulfate (SDS) micelles) [33–35]. This structural rearrangement has a strong impact on Cu^{2+} binding modes in terms of both donor atoms and affinity. The copper interactions strongly depend on the peptide backbone structure. Although most of the studies show that PrP amyloidogenic region mediates membrane interaction, the behavior of the octarepeat region in presence of micelles and Cu^{2+} ions was investigated as well. So far, it has not been proven that the octarepeat fragment embeds in membranes, but it has been suggested by several molecular dynamics calculations [36,37]. In this work, we have investigated Cu^{2+} binding features of the human octapeptide repeat (human Octa$_4$, hPrP$_{60–91}$) (Ac-PHGGGWGQPHGGGWGQPHGGGWGQ-PHGGGWGQ-NH_2) and chicken hexapeptide repeat (chicken Hexa$_4$, chPrP$_{54–77}$) (Ac-HNPGYPHNPGYPHNPGYPHNPGYP-NH_2) fragments in a mixed DMSO-water solution and in the presence of micelles formed by anionic sodium dodecyl sulfate (SDS) surfactant. As mentioned, the flexible N-terminal domain of the prion protein is believed to play a primary role in both trafficking of the protein through the cell membrane and its pathogenic conversion into the *β*-sheet-rich scrapie isoform (PrP^{Sc}). We focused on the N-terminal repeated sequences of prion proteins to understand the bioinorganic chemistry of biologically significant copper complexes of the N-terminal domain of the human prion protein (hPrP), in the presence of micelles, which mimic the lipid bilayer, to which the hPrP is anchored to in vivo. Due to the presence of a hydrophobic domain in N-terminal domain and the ability of the prion protein to interact with the lipid bilayer, the physiochemical research was carried out in the presence of surfactant (SDS) mimicking the membrane environment in vitro. We also compared our results with the ones previously obtained for amyloidogenic human and chicken fragments in micelle environment. Moreover, octa and hexa repeated fragments are stronger ligands for Cu^{2+} ions than the amyloidogenic regions of both human and chicken. For these reasons understanding their behavior in water and micelle environment is very interesting. The main objective of this work was to understand effects of metal ion and lipid bilayer on the structural rearrangements of human octapeptide and chicken hexapeptide N-terminal domain.

2. Experimental

2.1. Materials

The N- and C-terminally protected human octapeptide repeat (human Octa$_4$, hPrP$_{60–91}$) (Ac-PHGGGWGQPHGGGWGQPHGGGW-GQPHGGGWGQ-NH_2) and chicken hexapeptide repeat (chicken Hexa$_4$, chPrP$_{54–77}$) (Ac-HNPGYPHNPGYPHNPGYPHNPGYP-NH_2) fragments were purchased from KareBayBiochem (USA) (certified purity: 98%) and used as received. Their purity was checked potentiometrically. Cu$(ClO_4)_2$ was extra pure product (Sigma-Aldrich); concentration of its stock solutions was determined by ICP-MS. The carbonate-free stock solution of 0.1 M NaOH was potentiometrically standardized with potassium hydrogen phthalate (both Sigma-Aldrich). All samples were prepared with freshly doubly distilled water. The ionic strength (*I*) was adjusted to 100 mM and 40 mM by addition of $NaClO_4$ and SDS respectively (Sigma Aldrich).

2.2. Potentiometric measurements

Potentiometric measurements were performed at constant temperature of 298 K under argon atmosphere using a MOLSPIN pH-meter. Stability constants both for protons and Cu^{2+} complexes were calculated from titrations carried out over the range pH 2–11 using a total volume of 1.5 ml. NaOH was added from 0.5 ml micrometer syringe. Before each measurement, the electrode was calibrated by titration of $HClO_4$ (4 mM) with a strong base. The titrations of ligand and complexes were performed in mixes DMSO-water (30:70, v/v) solution of 4 mM $HClO_4$ at 100 mM $NaClO_4$ ionic strength and in water solution of 4 mM $HClO_4$ at 40 mM SDS ionic strength. Purities and the exact concentrations of ligand solutions were determined by the Gran method [38,39]. The ligand concentrations were 0.5 mM, the Cu^{2+} to ligand molar ratios were 1:1.1. The SUPERQUAD program was used for stability constant calculations [38]. Reported log β values refer to the overall equilibria:

$$pCu + qH + rL = Cu_pH_qL_r \quad (1)$$

$$\beta = \frac{[Cu_pH_qL_r]}{[Cu]^p[H]^q[L]^r} \quad (2)$$

Charges are omitted for clarity; $\log K_{step}$ values refer to the protonation process:

$$Cu_pH_{q-1}L_r + H = Cu_pH_qL_r \quad (3)$$

(charges omitted; p might also be 0). The speciation diagrams were plotted with the HYSS 2006 program [40].

2.3. UV–Vis measurements

The absorption spectra were recorded on a Cary 300 Bio spectrophotometer in the 800–200 nm range. Measurements were performed for 3 ml sample in quartz cell of the 1 cm pathlength. The final peptide concentration was 1 mM, the metal to ligand molar ratio was 1:1.1. The solutions were prepared in mixes DMSO-water (30:70, v/v) solution of 4 mM $HClO_4$ at 100 mM $NaClO_4$ ionic strength and in water solution of 4 mM $HClO_4$ at 40 mM SDS ionic strength. Data were processed using Origin 7.0.

2.4. Circular dichroism measurements

Circular dichroism (CD) spectroscopy experiments were performed on a spectropolarimeter Jasco J-1500 at 298 K in a 0.01 cm and 1 cm quartz cell. The spectral range was 180–300 and 200–800 nm, respectively. The solutions were prepared in mixes DMSO-water (30:70, v/v) solution of 4 mM $HClO_4$ at 100 mM $NaClO_4$ ionic strength and in water solution of 4 mM $HClO_4$ at 40 mM SDS ionic strength. Ligand concentration was 1 mM (200–800 nm range) or 0.1 mM (180–300 nm range); Cu^{2+} to ligand molar ratio was 1:1.1. The direct CD measurements (Θ) were converted to mean residue molar ellipticity (Δε) using Jasco Spectra Manager.

Table 1
Thermodynamic and spectroscopic parameters for Cu^{2+} complex formation of human $Octa_4$ at 298 K in A) mixed DMSO-water (30:70, v/v) solution and B) 40 mM SDS solution. Standard deviation on the last significant figure on parenthesis.

Species	logβ	pKa	logK*	UV–Vis		CD	
				λ [nm]	ε [$cm^{-1}M^{-1}$]	λ [nm]	Δε [$cm^{-1}M^{-1}$]
A) 30%DMSO							
CuH_2L	18.63 (5)		5.59				
CuHL	13.74 (5)	4.89	6.95				
CuL	9.16 (3)	4.58		608	48.78	586.8	0.07
						343.1	0.05
$CuH_{-2}L$	−3.98 (5)			605	110.58	590.8	0.24
						341.8	0.18
$CuH_{-3}L$	−12.46 (8)	8.48		590	129.53	589.7	0.29
						500.4	−0.11
						336.0	0.18
$CuH_{-4}L$	−21.94 (9)	9.48		557	140.28	589.2	0.41
						504.1	−0.38
						329.5	0.38
B) SDS							
CuH_2L	22.28 (3)		6.91				
CuHL	16.11 (3)	6.17	8.05	629	125.42	603	0.15
						341.7	0.05
CuL	9.52 (6)	6.59		616	161.88	595.5	0.37
						340.2	0.25
$CuH_{-2}L$	−6.89 (8)			606	198.63	594.7	0.59
						341.1	0.62
$CuH_{-3}L$	−16.48 (13)	9.59		548	218.63	611	0.16
						333.7	0.68
$CuH_{-4}L$	−25.43 (10)	8.95		537	258.07	599.1	0.12
						504	−0.24
						328	0.60

2.5. NMR experiments

NMR experiments were carried out at 298 K using a 600 MHz Bruker Advance spectrometer. NMR spectra were processed with TopSpin 3.6 software and analyzed with the program CARA [41]. Suppression of residual water signal was achieved by excitation sculpting [42], using a selective 2 ms long square pulse on water. Proton resonance assignment was achieved by 2D NMR analysis, ^1H-^1H TOCSY and NOESY. The peptides were dissolved in 20 mM phosphate buffer at pH 7.4 with 10% of D_2O and 40 mM SDS. The final peptide concentration was 0.5 mM. The desired concentrations of Cu^{2+} ions and SDS were obtained by using stock solutions of $Cu(NO_3)_2$ and deuterated SDS (Sigma Chemical Co.) in D_2O.

3. Results and discussion

3.1. Thermodynamic stability constants of Cu^{2+}-human $Octa_4$ complexes

The thermodynamic parameters of human $Octa_4$ $hPrP_{60–91}$ in mixed DMSO-water (30:70, v/v) and sodium dodecyl sulfate (SDS) solutions are collected in Table 1S. Human $Octa_4$ is poorly soluble in pure water and the measurements were performed in DMSO-water mixed solvent, which is a good mimic of a crowded cell, since it is more defense than water. The obtained data indicate that human $Octa_4$ behaves as H_4L acid. The four protonation constants correspond to consecutive proton binding to imidazole nitrogens of four histidine residues: His61, His69, His77 and His85 [9–11,43]. In presence of SDS micelles, the protonation constants are higher than those in water solution (mixed DMSO-water (30:70, v/v) solution of 4 mM $HClO_4$ at 100 mM $NaClO_4$ ionic strength). The difference results from the fact that the imidazole nitrogen atoms are more basic in SDS (higher pK values), which might be the consequence of the interaction of the imidazole rings with the anionic surfactant. This effect has been previously observed for other histidine containing peptides [33,44].

Potentiometric titrations of Cu^{2+}-human $Octa_4$ complexes in mixed DMSO-water (30:70, v/v) solution and in the presence of SDS micelles were carried out to evaluated the corresponding complex formation constants and the distribution diagrams (Table 1, Fig. 1). In the equimolar Cu^{2+}-human $Octa_4$ DMSO-water solution the set of complexes formed consists of six species: CuH_2L, CuHL, CuL, $CuH_{-2}L$, $CuH_{-3}L$, $CuH_{-4}L$. In SDS solutions, the most accurate fit of titration curves for the Cu^{2+}-human $Octa_4$ complexes also indicates the presence of six equimolar species: CuH_2L, CuHL, CuL, $CuH_{-2}L$, $CuH_{-3}L$, $CuH_{-4}L$. The stability constants for the same species in DMSO-water and SDS solution distinctly differ. At pH around 7, the main species are CuL and $CuH_{-2}L$ species in DMSO-water solution (Fig. 1A), while in SDS micelles, CuL complex dominates (Fig. 1B). The first species CuH_2L results from two histidine imidazole deprotonation. The essential difference between logK* values ($log\beta^*CuH_2L - log\beta^*H_2L$) measured in DMSO-water (5.59) and SDS (6.91) (Table 1) can be explained by the fact that imidazole nitrogen atoms are more basic in SDS solution and they deprotonate at higher pH values than in case of DMSO-water solution. Further deprotonation results in the formation of CuHL species in which three imidazole nitrogen atoms of His residues are deprotonated. The logK* of this species in DMSO-water solution differs by 1.36 units, which indicate that the Cu^{2+} ion may coordinate to three imidazoles. Independently on the solvent, for CuL species we observed the decrease of p*Ka* of the copper complex in comparison to the free ligand (Table 1), indicating the involvement of an additional imidazole nitrogen atom in the metal coordination sphere. The next complex species ($CuH_{-2}L$, $CuH_{-3}L$, $CuH_{-4}L$ for DMSO-water and SDS solution) results from the deprotonation of amide nitrogen atoms.

3.2. Spectroscopic features of Cu^{2+}-human $Octa_4$ in DMSO-water and SDS environment

All spectroscopic data including CD and UV–Vis experiments are shown in Table 1. The results obtained by spectroscopic studies (UV–Vis and CD spectra) of human $Octa_4$ in DMSO-water and SDS solutions are shown in Figs. 1S and 3, respectively.

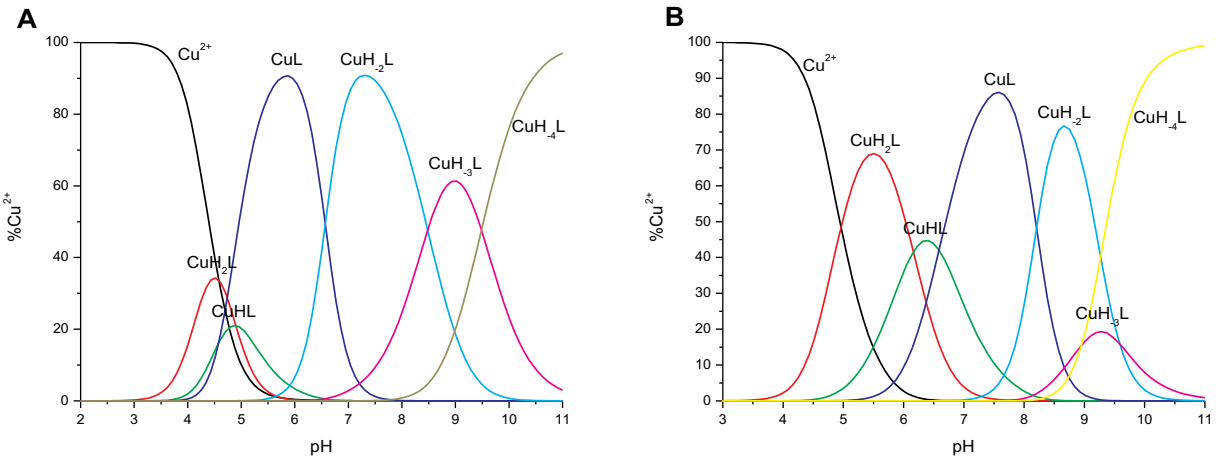

Fig. 1. Species distribution diagram for Cu^{2+}-human $Octa_4$ complexes at 1:1.1 Cu^{2+}/peptide ratio in A) mixed DMSO-water (30:70, v/v) solution and B) 40 mM SDS solution. T = 298 K, $c_{peptide}$ = 0.5 mM (for clarity, the charges on the speciation plots were omitted).

3.2.1. DMSO-water

The first complex detected by UV–Vis and CD spectra is CuL, with a maximum concentration at pH 6 (Fig. 1A). At this pH, a UV–Vis d-d band at 608 nm and a CD d-d band at 586.8 nm are observed (Figs. 1SA, 2SA and Table 1). These values together with potentiometric parameters support a 4N donor set ($4N_{im}$) [45,46]. The involvement of imidazole nitrogens is confirmed also by the characteristic charge transfer transitions detected in CD spectra at 343.1 nm for $N_{im} \rightarrow Cu^{2+}$ (LMCT transition originating from the π1 orbital of the imidazole ring to Cu^{2+}) absorptions (Table 1, Fig. 2SA).

$CuH_{-2}L$, which dominates at pH 7.5 (Fig. 1A), has a 4N copper binding mode as well. d-d transition band at 590 nm has significantly increased (Fig. 2SA, Table 1), which corresponds to amide nitrogen in $CuH_{-2}L$ complex having metal ion bound to an $\{2N_{im}, 2N^-\}$ donor set. The appearance of negative absorption band on CD spectra at around 500 nm (Fig. 2SA) at pH 9 ($CuH_{-3}L$ form) with the simultaneous shift of the d-d band from 605 to 590 nm on UV–Vis spectra (Fig. 1SA) strongly support additional amide coordination indicating a $\{N_{im}, 3N^-\}$ donor set. At pH above 9, the differences observed in the UV–Vis and CD spectra support coordination with further amide nitrogen. For $CuH_{-4}L$ the coordination mode $\{4N^-\}$ is supported by the shift of the d-d band from 590 to 557 nm (Fig. 1SA) and appearance of intense d-d band at around 500 on CD spectra (Fig. 2SA).

3.2.2. SDS

In the case of SDS, CuL is the dominant species at pH 7.5 (Fig. 1B). CD spectra have one positive band at 340.2 nm which is commonly assigned to the $N_{im} \rightarrow Cu^{2+}$ charge transfer transition and a positive band at 595.5 nm (Fig. 2SB, Table 1). A d-d band at 616 nm is observed in the UV–Vis spectra (Fig. 1SB). These findings strongly suggest a $\{3N_{im}\}$ binding mode. The next $CuH_{-2}L$ species dominates at 8.5 (Fig. 1B). Increase of d-d band at 595 nm and charge transfer band at 340 nm on CD spectra (Fig. 2SB) with the simultaneous appearance of d-d band at 606 nm in the UV–Vis spectra indicate a $\{2N_{im}, 2N^-\}$ binding mode with 2 imidazole nitrogens and two amide nitrogen involved in copper binding sphere (Fig. 1SB). The $CuH_{-3}L$, which dominates at pH 9.5 (Fig. 1B) has a 4N copper binding mode as well; the binding of an additional amide nitrogen is confirmed by the shift of the d-d band to 548 nm in the UV–Vis spectra (Fig. 2SB). The coordination of the next amide nitrogen occurs at pH around 10.5 (dominant $CuH_{-4}L$ complex form) which is supported by appearance of negative absorption band at 504 nm in the CD spectra (Fig. 2SB). The shift of the d-d band to 537 nm on UV–Vis spectra also supports 4N binding mode (Fig. 1SB).

3.3. Influence of SDS micelles on human $Octa_4$ and Cu^{2+}-$Octa_4$ conformation

In DMSO-water solution, apo human $Octa_4$ fragment has CD spectra characterized by strong negative absorption band at around 197 nm and positive absorption band at around 225 nm over all the pH range (Fig. 2). This conformation is not trivial. In literature, such distribution of near CD bands is called PolyProline II (PPII) conformation, which is associated with proline residues repeated four times in the investigated sequence. This conformation shows a left-handed helix, typical of the collagen triple-helix structures [47], but now it is present conformations of polypeptide chain in folded proteins. The PPII helix occurs frequently in natural polypeptides and globular proteins [48–50]. Interestingly, it is also observed for polypeptides that are not necessarily dominated by proline, or even do not contain proline [51,52]. A 197 nm negative and 225 nm positive absorption bands indicate that the peptides are not fully unstructured but may adopt a regular extended helical conformation close to the three fold PPII left-handed helix, short stretches of which are interspersed with turns and bends [53]. In case of Cu^{2+}-human $Octa_4$ complexes, the near CD spectra looks different than for the apo peptide. It means that adding copper ions into the investigated system may induce some essential conformational changes. On the CD spectra (Fig. 2B) the positive absorption band at 230 nm is shifted with respect to the apo peptide. The position of the negative absorption bands is also different – it is located in 185–195 nm range. Interestingly, for copper complexes over the pH range 7.30 to 11 (Fig. 2B), an additional band at 215 nm is observed, together with a simultaneous decrease of the band at 230 nm. This indicates that copper ions might influence the structural features of the investigated ligands.

The conformation of the human $Octa_4$ ligand in the presence of SDS micelles differs from the one observed in DMSO-water solution. Over the pH range 2–7, two absorption bands are present: a negative one at 205 nm and positive one at 225 nm (Fig. 3A). The negative band at 205 nm is shifted relative to band indicated on PolyProline II conformation observed in case of ligand in DMSO-water solution. On the other hand, the positive absorption band at 225 nm is located at the same wavelength as in DMSO-water solution. Some conformational changes are observed over the pH range 8–11 (Fig. 3A). The positive band is shifted from 225 to 230 nm with simultaneous decrease of intensity. Moreover, the appearance of two negative absorption bands at 205 and 220 nm, indicates the presence of α-helix structural elements (Fig. 3A). For Cu^{2+}-human $Octa_4$ complexes a very similar situation is observed. At pH 2–7.5 a negative absorption band at 205 nm and a positive band at 225 nm are present (Fig. 3B). From pH 8 to 11, the structure of the peptide backbone changes to a typical α-helical

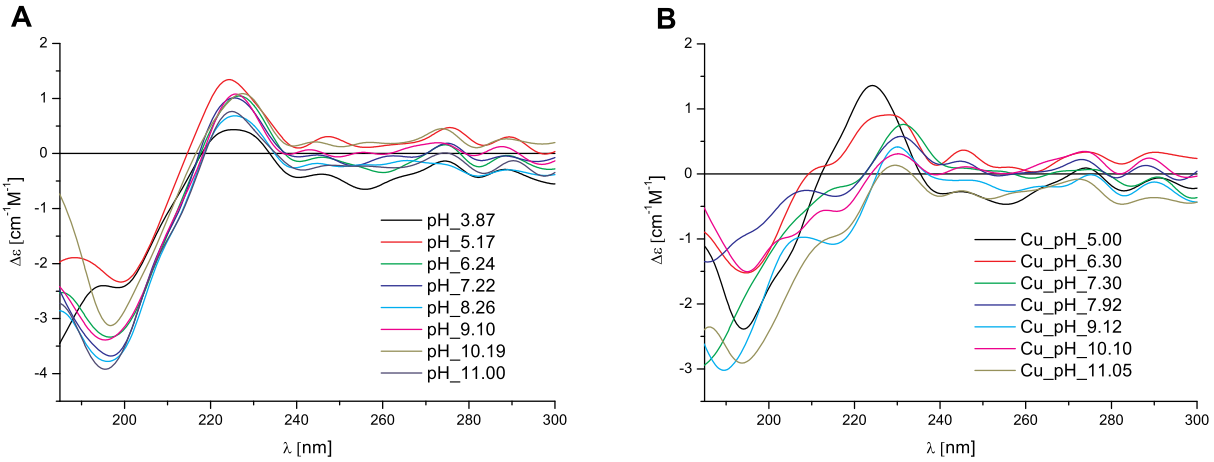

Fig. 2. Near CD spectra for A) ligand human $Octa_4$ and B) Cu^{2+}-human $Octa_4$ complex in mixed DMSO-water (30:70, v/v) solution in 0.01 cm quartz cell. 1:1.1 Cu^{2+}/peptide ratio, T = 298 K, $c_{peptide}$ = 0.1 mM.

structure (not PPII), as indicated by two negative absorption bands at 203 nm and 215 nm with simultaneous disappear once of the positive absorption band at 225 nm (Fig. 3B).

In order to get more insights into the 3D structure of human $Octa_4$, we recorded NMR spectra in the absence and in presence of SDS. The interaction between micelles and human $Octa_4$ is supported by the detection of chemical shift variations of proton resonances in the two different environments (Fig. 3S).

In order to identify secondary structure elements, we performed 2D ^1H-^1H NOESY experiments. The analysis of the obtained spectra confirms the role played by SDS micelles in inducing specific structural rearrangements of the peptide backbone. In particular, the presence of not trivial NH-NH NOEs correlations between adjacent amide protons supports the formation of backbone conformational rearrangement (Fig. 4). Unfortunately, the superimposition and the proximity between the signals belonging to identical amino acids of the different repeats prevents the detection of NOE connections from αN, αNi + 2, or αNi + 3, typical of α-helix structure.

3.4. Thermodynamic stability constants of Cu^{2+}-chicken $hexa_4$ complexes

The thermodynamic parameters for chicken hexapeptide repeat fragment, chicken $Hexa_4$ $chPrP_{54–77}$, in DMSO-water (30:70, v/v) and SDS solutions are collected in Table 2S. Similar to human $Octa_4$, chicken $Hexa_4$ is poorly soluble in pure water and the measurements were performed in DMSO-water mixed solvent. The obtained data indicate that chicken $Hexa_4$ behaves as a H_8L acid. The four protonation constants correspond to consecutive proton binding to the phenolic group of tyrosine residues and following four imidazole nitrogens of histidine residues (His54, His60, His66, His72). In the presence of SDS micelles, pKa values for histidine residues are higher (around 1.5 units) than in the DMSO-water solution and the last two constants of tyrosine residues are indistinguishable.

According to potentiometric data, the chemical species formed in both DMSO-water and SDS solutions are the same, although their stability constants differ distinctly (Table 2). Species distribution profiles for Cu^{2+} complexes of chicken $Hexa_4$ in DMSO-water and SDS solutions are collected in Fig. 5. In the equimolar Cu^{2+}-chicken $Hexa_4$ DMSO-water solutions, the set of complexes formed consists of nine species: CuH_6L, CuH_5L, CuH_4L, CuH_3L, CuH_2L, CuHL, CuL, $CuH_{-1}L$, $CuH_{-2}L$ (Fig. 5A). In SDS solution, the most accurate fit of titration curves indicates the presence of eight equimolar species: CuH_6L, CuH_5L, CuH_4L, CuH_3L, CuH_2L, CuHL, CuL, $CuH_{-2}L$ (Fig. 5B). The stability constants for the same species in SDS solution are higher than those found in DMSO-water. At pH around 7, CuH_3L and CuH_2L are the main species for both DMSO-water and SDS solutions. The first formed complex, CuH_6L results from the deprotonation of two histidine imidazole. The enormous difference between logK* values ($log\beta^*CuH_6L - log\beta^*H_6L$)

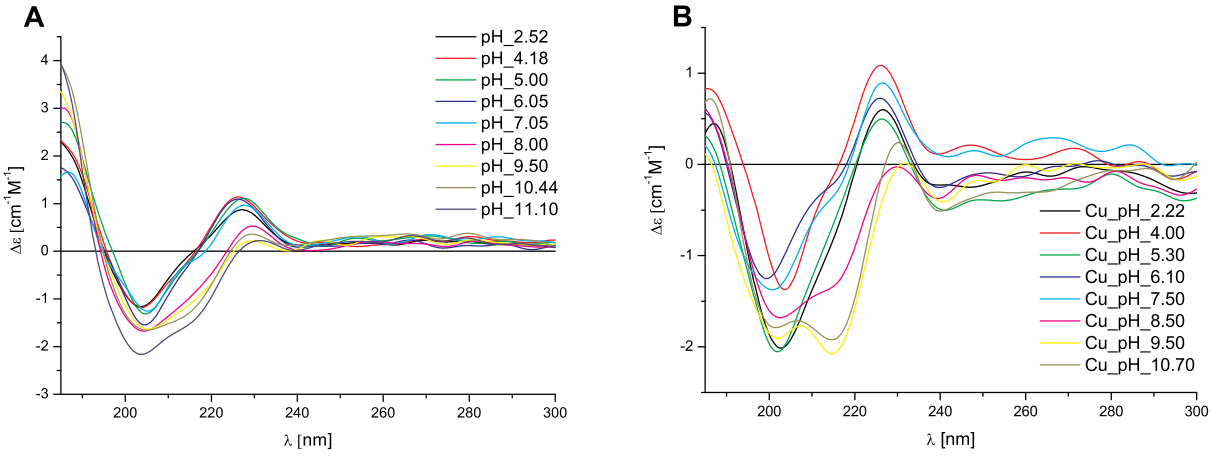

Fig. 3. Near CD spectra for A) ligand human $Octa_4$ and B) Cu^{2+}-human $Octa_4$ complex in 40 mM SDS solution in 0.01 cm quartz cell. 1:1.1 Cu^{2+}/peptide ratio, T = 298 K, $c_{peptide}$ = 0.1 mM.

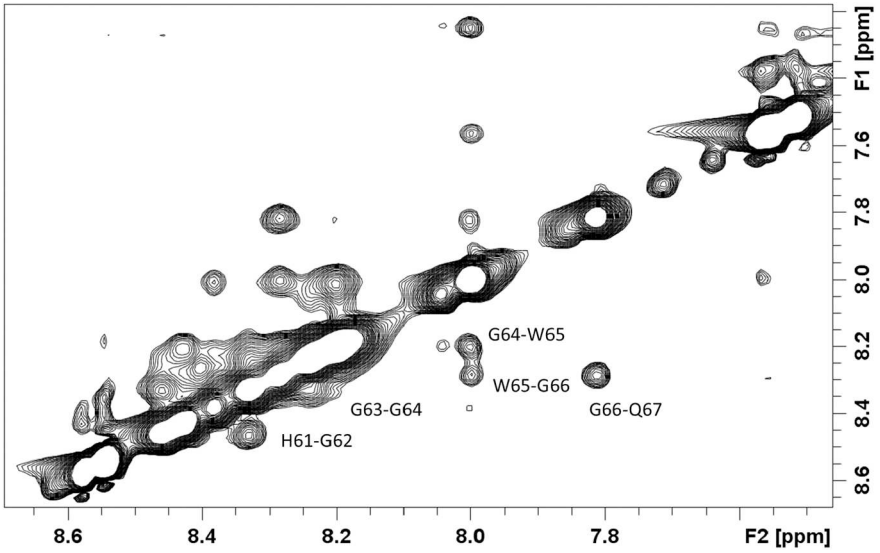

Fig. 4. Amide region of ^{1}H-^{1}H NOESY spectrum of human $Octa_4$ 0.5 mM in presence of SDS micelles. Selected NH-NH connectivities are shown, the residues numbering is reported as just an example. No distinction between octarepeat is obtained.

Table 2
Thermodynamic and spectroscopic parameters for Cu^{2+} complex formation of chicken $Hexa_4$ at 298 K in A) mixed DMSO-water (30:70, v/v) solution and B) 40 mM SDS solution. Standard deviation on the last significant figure on parenthesis.

Species	logβ	pKa	logK*	UV–Vis		CD	
				λ [nm]	ε [$cm^{-1}M^{-1}$]	λ [nm]	Δε [$cm^{-1}M^{-1}$]
A) 30%DMSO							
CuH_6L	59.13 (4)		5.57				
CuH_5L	55.18 (1)	3.95	7.80	650	43.40		
CuH_4L	50.34 (1)	4.84	9.62	629	58.16	583	0.10
						329.6	−0.07
CuH_3L	43.89 (2)	6.45		622	65.66	579.2	0.10
						342.7	−0.09
CuH_2L	37.06 (3)	6.83		622	84.41	564.3	0.09
				389	324.49	376.7	−0.29
						294	0.10
CuHL	28.36 (4)	8.70		622	92.44	571.8	0.07
				389	410.49	378.3	−0.34
						293.1	0.26
CuL	19.25 (4)	9.11		621	100.12	379	0.37
				386	453.27	293.1	0.50
$CuH_{-1}L$	9.34 (7)	9.91		621	107.72	580	−0.22
						362.6	−0.34
						294.7	0.70
$CuH_{-2}L$	−0.36 (5)	9.70		588	106.03	555.3	−0.59
						378.2	−0.42
						320.3	1.1
B) SDS							
CuH_6L	62.11 (2)		7.73				
CuH_5L	56.65 (2)	5.46	9.89				
CuH_4L	51.04 (3)	5.61	12.34	668	71.25	599.4	0.05
						334.7	−0.05
CuH_3L	44.84 (2)	6.20		612	127.44	582.3	0.04
						297.4	−0.33
CuH_2L	37.88 (3)	6.96		612	149.61	320.3	−0.29
				387	563.00		
CuHL	29.18 (4)	8.70		595	138.86	593.4	−0.17
				387	459.56	356.7	−0.22
CuL	19.79 (5)	9.39		568	138.74	556	−0.50
						365.1	−0.41
						312	0.83
$CuH_{-2}L$	0.43 (5)			568	123.76	640.4	0.05
						550.3	−0.27
						328.7	1.52

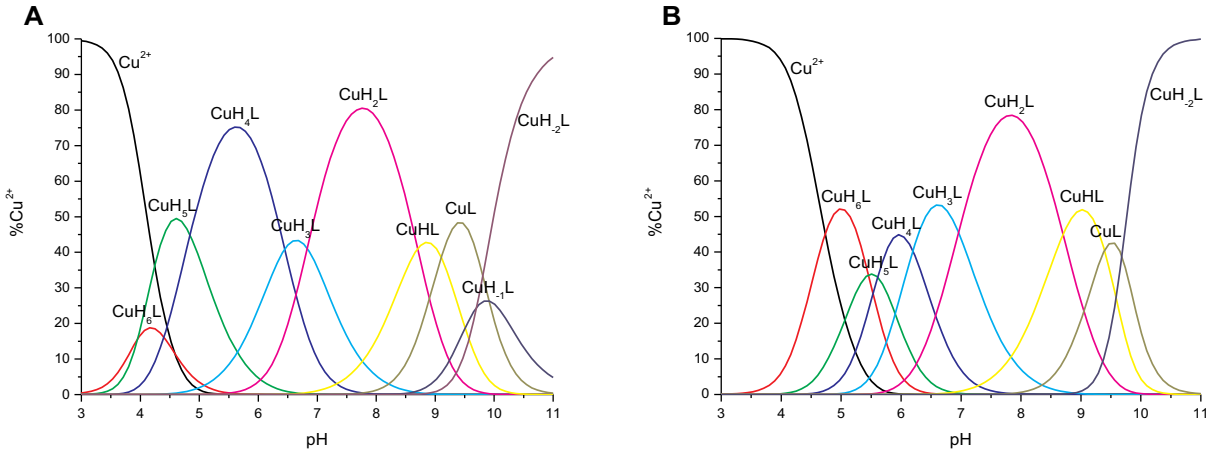

Fig. 5. Species distribution diagram for Cu^{2+}-chicken $Hexa_4$ complexes at 1:1.1 Cu^{2+}/peptide ratio in A) mixes DMSO-water (30:70, v/v) solution and B) 40 mM SDS solution. T = 298 K, $c_{peptide}$ = 0.5 mM (for clarity, the charges on the speciation plots were omitted).

measured in DMSO-water (5.57) and SDS (7.73) (Table 2) is explained by the fact that imidazole nitrogen atoms are more basic in SDS solution and they deprotonate at higher pH values than in the case of DMSO-water solution. Further deprotonation results in the formation of CuH_5L species in which three imidazole nitrogen atoms of His residues are deprotonated. The logK* of these species in DMSO-water and SDS solution differs by 2.23 and 2.16 units respectively, which indicate that the Cu^{2+} ion may coordinate to three imidazoles (Table 2). For CuH_4L species in both DMSO-water and SDS solutions we observed the decrease of the p*Ka* of the copper complex in comparison to the free ligand (Table 2), indicating the involvement of additional imidazole nitrogen atoms in the coordination sphere. Moreover, the high logβ* of these species in DMSO-water and SDS solutions (9.62 and 12.34 respectively) suggest four imidazole nitrogen atoms in the coordination sphere. The next complex species ($CuH_{-1}L$ and $CuH_{-2}L$) result from the deprotonation of amide nitrogen atoms, which replace imidazole nitrogen atoms from metal coordination sphere.

3.5. Spectroscopic features of Cu^{2+}-chicken $Hexa_4$ in DMSO-water and SDS environment

All spectroscopic data including CD and UV–Vis experiments are presented in Table 2. The results obtained by spectroscopic studies (UV–Vis and CD spectra) of chicken $Hexa_4$ in DMSO-water and SDS solutions are shown in Figs. 4S and 9, respectively.

3.5.1. DMSO-water and SDS

The first complex detected by UV–Vis and CD spectra is the CuH_4L species, with a maximum concentration at pH 5.5 (Fig. 5A). At this pH, a UV–Vis and CD d-d bands centered at 629 nm and 583 nm, respectively, are observed (Fig. 4SA, 5SA Table 2). In the CD spectra an additional charge transfer transitions band ($N_{im} \rightarrow Cu^{2+}$) at 329.6 nm is evident (Fig. 5SA, Table 2). These values, together with the results of potentiometric measurements, indicate a 4N donor set ($4N_{im}$). In the pH range 5.5–10 (CuH_3L, CuH_2L, CuHL, CuL) no significant changes on UV–Vis and CD spectra are observed, indicating the presence of the same copper binding mode. At pH 10–12 ($CuH_{-1}L$, $CuH_{-2}L$) we observed intense negative absorption band at 554–598 nm range on CD spectra due to the replacement of imidazole by amide nitrogens in coordination sphere. Interestingly, the same copper coordination mode for Cu^{2+}-chicken $Hexa_4$ in SDS solution is observed (Table 2), but the same chemical species formed in SDS solutions are present at higher pH (around 0.5 units) with respect to those found in DMSO-water solution (Fig. 5).

3.6. The effect of SDS micelles and copper ions on structural conformation of chicken $Hexa_4$

The near CD of the apo chicken $Hexa_4$ ligand in DMSO-water solution is shown in Fig. 6A. In the pH range 4–11, two negative absorption bands at 202 nm and 216–219 nm and a positive low intensive

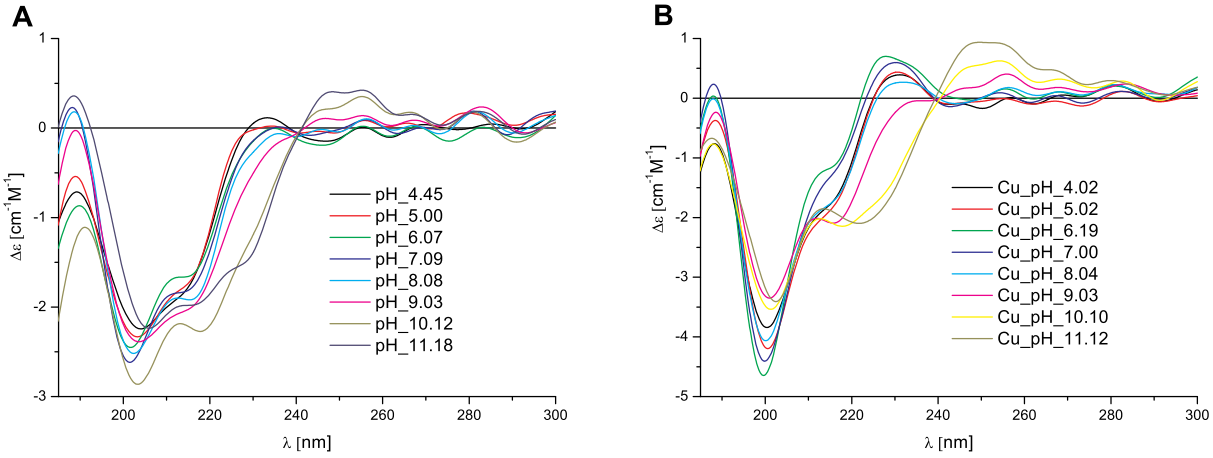

Fig. 6. Near CD spectra for A) ligand chicken $Hexa_4$ and B) Cu^{2+}-chicken $Hexa_4$ complex in mixes DMSO-water (30:70, v/v) solution in 0.01 cm quartz cell. 1:1.1 Cu^{2+}/peptide ratio, T = 298 K, $c_{peptide}$ = 0.1 mM.

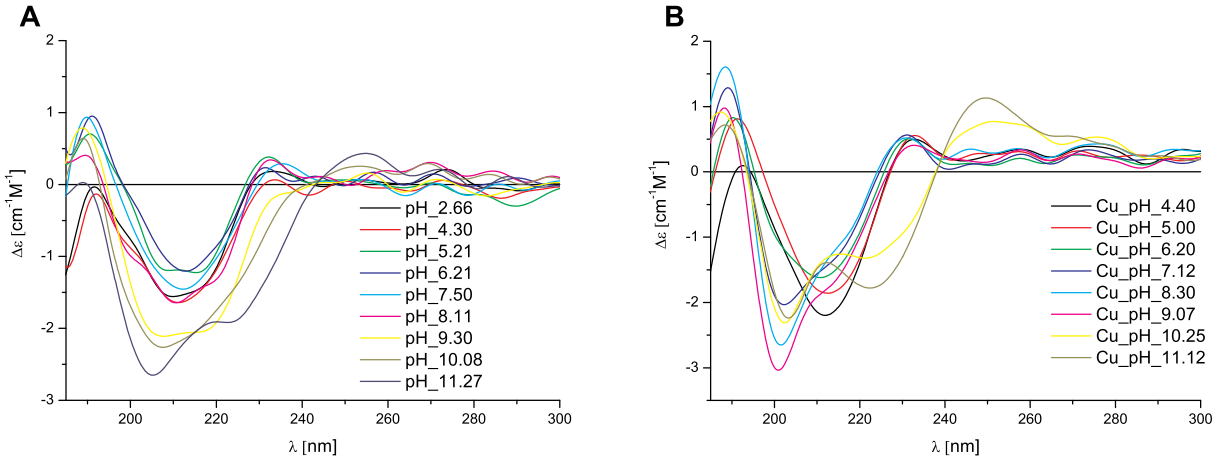

Fig. 7. Near CD spectra for A) ligand chicken $Hexa_4$ and B) Cu^{2+}-chicken $Hexa_4$ complex in 40 mM SDS solution in 0.01 cm quartz cell. 1:1.1 Cu^{2+}/peptide ratio, T = 298 K, $c_{peptide}$ = 0.1 mM.

band at 230 nm are present on near CD spectra. These bands can suggest some α-helical structure of the peptide backbone. At pH above 9, some changes on CD spectra are observed – two negative absorption bands are shifted to high wavelengths, positive low intensive band at 230 nm disappears together with the simultaneous appearance of new positive absorption band at 250 nm. For Cu^{2+}-chicken $Hexa_4$ complexes (Fig. 6B) CD spectra shows some significant differences to that one observed for ligand (Fig. 6A). In pH range 4–9, the negative absorption band at 200 nm and the negative less intense absorption band at 220 nm are observed. At pH above 9, negative band at 220 nm becomes much more intensive, indicating on α-helical structure of the peptide backbone. It means that some structural changes after adding copper ions are observed. The conformation of α-helix might be changed at a certain extent (Fig. 6B).

In order to compare structural properties of chicken $Hexa_4$ ligand and its copper complexes in micelle environment, near CD spectra in SDS solution were recorded (Fig. 7). As shown in Fig. 7A, over the pH range 2.5–7.5, the CD spectra of the apo ligand are characterized by two absorption bands: a negative one at 212 nm and a positive one at 230 nm. From pH 8 to 11, two negative absorption bands at 206 nm and 222 nm are present, with a simultaneous shift of the positive absorption band at 230 nm to 250 nm. This indicates that the investigated ligand adopts typical α-helix structure at higher pH values. Upon Cu^{2+}addition to chicken $Hexa_4$ different CD bands are detected at pH 7–8. At pH around 7 the apo ligand are characterized by one negative absorption band at 212 nm, while copper complexes results in two negative absorption bands characteristic for helical structure (Fig. 8). This may indicate that at physiological pH, in SDS micelle environment, copper ions have an impact on the structure of the apo ligand.

Fig. 8. Near CD spectra of chicken $Hexa_4$ 0.1 mM at pH 7, 40 mM SDS, in the absence (red line) and presence of Cu^{2+} (black line). Metal to ligand ratio 1:1.1. (For interpretation of the references to color in this figure legend, the reader is referred to the web version of this article.)

3.7. Human $Octa_4$ vs chicken $Hexa_4$

In order to evaluate the complex stability of both ligands in the two different environments the competition plots were used. They are based on the calculated formation constants and describe a hypothetical situation, in which equimolar amounts of the metal ion and two ligands (human $Octa_4$ and chicken $Hexa_4$) are present in solution at different pH values (Figs. 9–11). Our findings indicate that chicken $Hexa_4$ fragment is a better copper ligand than human $Octa_4$, both in DMSO-water and SDS solutions (Fig. 9). We observed a similar situation for the amyloidogenic region of both human and chicken prion protein. The chicken fragment revealed a higher stability than its human analogue over all the studied pH range [35]. This behavior is probably due to the stabilizing effect of the aromatic ring of tyrosine residue on copper binding in both analyzed systems. Moreover, in SDS environment, both ligands indicate different copper coordination modes. For the human $Octa_4$ fragment three histidine residues are anchoring sites for copper ions, while for the chicken $Hexa_4$ four histidine residues are involved in binding. In SDS solution, at pH above 10 the situation changes. Human $Octa_4$ forms more stable copper complexes. This may result from the fact that the amide nitrogens are coordinated to the metal ion in the $CuH_{-4}L$ complex, which most likely involves five nitrogens in binding.

We also wanted to understand the impact of SDS micelle environment, which is a good membrane mimic, on the stability of the human $Octa_4$ and chicken $Hexa_4$ complexes with Cu^{2+} ions (Fig. 10). The human $Octa_4$ ligand forms more stable copper complexes in mixed DMSO-water until pH 8 (Fig. 10A). This results from the number of imidazole nitrogen atoms involved in copper (II) binding. In case of DMSO-water environment four histidine residues are coordinated to Cu^{2+}, while in SDS micelles, only three His residues are engaged in metal binding. At above pH 8, human $Octa_4$-copper complexes are more eager to form in SDS, rather than in DMSO-SDS solution, because at this pH, the human $Octa_4$ fragment in presence of copper ions starts to form an α-helical structure (Fig. 3B), which may be more stable than PP II conformation observed in DMSO-water solutions (Fig. 2B). For chicken Cu^{2+}-$Hexa_4$ complexes, a similar behavior is observed (Fig. 10B). The comparison of the thermodynamic parameters obtained for the chicken

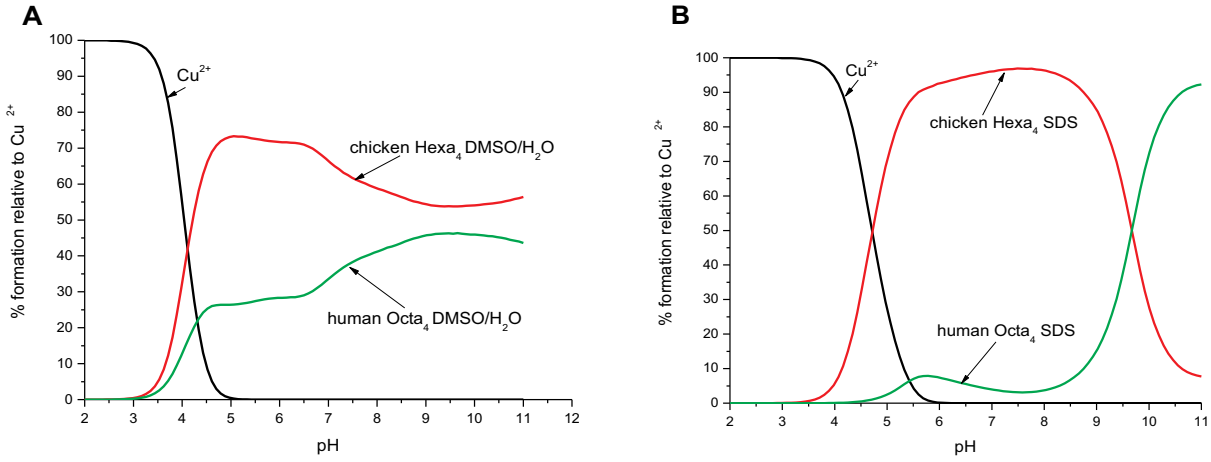

Fig. 9. Competition diagram between Cu^{2+}-human $Octa_4$ and Cu^{2+}-chicken $Hexa_4$ complexes in A) in mixed DMSO-water (30:70, v/v) solution and B) 40 mM SDS micelles. $[Cu^{2+}] = [Octa_4] = [Hexa_4] = 1$ mM.

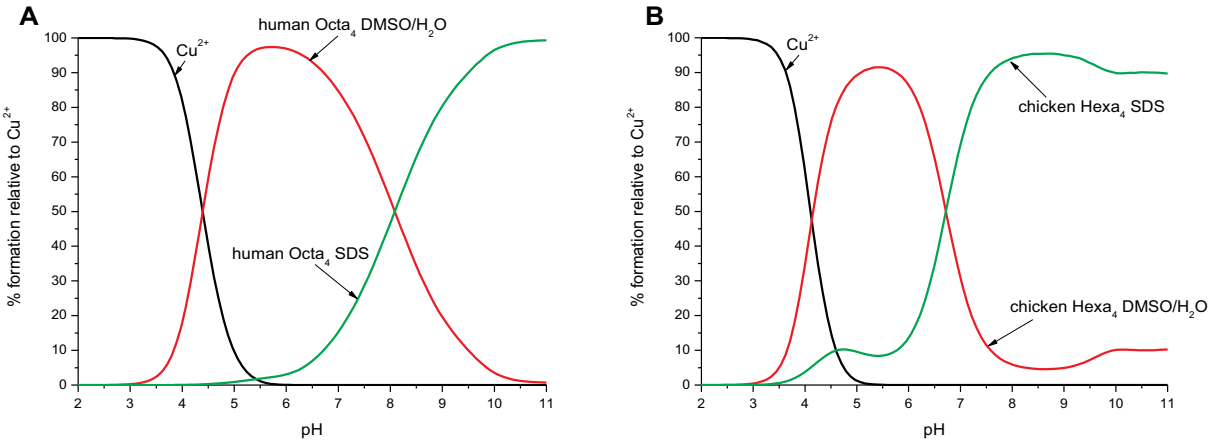

Fig. 10. Competition diagram between A) Cu^{2+}-human $Octa_4$ in DMSO-water and SDS solutions and B) Cu^{2+}-chicken $Hexa_4$. in DMSO-water and SDS solutions. $[Cu^{2+}] = [Octa_4] = [Hexa_4] = 1$ mM.

$Hexa_4$ fragment in two different environment points out that the chicken $Hexa_4$ is a stronger ligand for Cu^{2+} in DMSO-water solution up to pH 7. These differences may be associated with serious distinct arrangement of near CD absorption bands in DMSO-water and SDS environment (Figs. 6B and 10B respectively) resulting from different peptide backbone structure. On the other hand, over the pH range 7–11, chicken $Hexa_4$ copper complexes in SDS micelles are thermodynamically more stable than in DMSO-water solution. From the spectroscopic measurements it is known that copper binding mode for chicken $Hexa_4$ fragment in two different environments is very comparable. The differences result from the fact that addition of coper (II) ions to the investigated ligand at pH around 7 causes structural changes

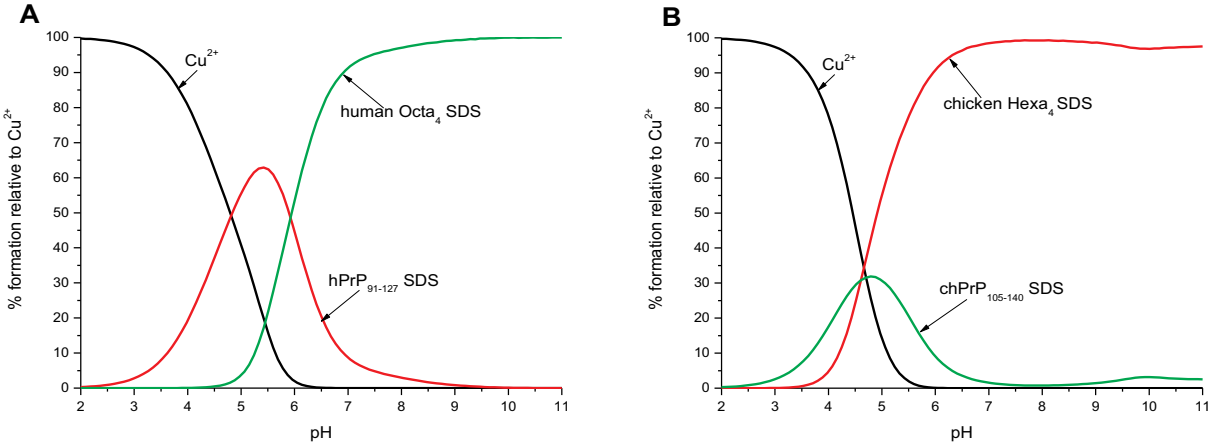

Fig. 11. Competition diagram between A) Cu^{2+}-human $Octa_4$ and Cu^{2+}-$hPrP_{91–127}$ in 40 mM SDS and B) Cu^{2+}-chicken $Hexa_4$ and Cu^{2+}-$chPrP_{105–140}$ in 40 mM SDS. $[Cu^{2+}] = [Octa_4] = [Hexa_4] = [hPrP_{91–127}] = [chPrP_{105–140}] = 1$ mM.

in the peptide backbone (Fig. 8), which starts to form an α-helix structure, while no conformational change in DMSO-water solution between apo and copper complexes is observed (Fig. 6).

4. Conclusion

In this paper, we studied copper(II) binding to the human ($Octa_4$, $hPrP_{60–91}$) and chicken ($Hexa_4$, $chPrP_{54–77}$) repeat regions located at N-terminal domain of prion proteins to clarify the role played by the histidine residues in the presence of sodium dodecyl sulfate (SDS) micelles, which are a mimic of membrane environment. The obtained results provide a fundamental first step in describing the thermodynamic and structural properties of Cu(II) binding to both human $Octa_4$ and chicken $Hexa_4$ repeats in both a DMSO/water and SDS micelle environment. In SDS environment, both ligands indicate different copper coordination modes, which results of the conformational changes in micelle environment. For the human $Octa_4$ fragment three histidine residues are anchoring sites for copper ions, while for the chicken $Hexa_4$ four histidine residues are involved in binding. We showed that α-helix structuring of the N-terminal prion protein domain influences both the copper coordination sphere and the copper binding affinity. Our findings also indicate that chicken $Hexa_4$ fragment is a better copper ligand than human $Octa_4$, both in DMSO-water and SDS solutions. This may be associated with aromatic ring of tyrosine residues present in chicken Hexa4 sequence, which stabilize copper anchoring site. We also compared the stability of Cu^{2+} complexes with human $Octa_4$ and chicken $Hexa_4$ with the corresponding amyloidogenic fragments derived from the human and chicken prion protein, respectively [33,35] (Fig. 11). At physiological pH, both human and chicken repeat fragments are more effective in copper binding than their amyloidogenic analogues in both environments. This comparison is well-understandable because of the fact that human and chicken repeat fragments contain four histidine residues acting as potential copper binding sites, while the amyloidogenic domain of the prion protein possess two copper binding sites located at H96 and H111 (in human analogue) and H110 and H124 (in the chicken one).

This finding is important for understanding the bioinorganic chemistry of prion proteins, showing a significant impact of membrane environment and Cu(II) binding ability on the structure of N-terminal prion protein domain, which can interact with lipid membrane in vivo The different structure in membrane environment and resulting from this different copper coordination mode of tandem repeats domain, may have a significant role in proteins misfolding and aggregation process.

Abbreviations

PrP	prion protein
PrPs	prion proteins
hPrP	human prion protein
chPrP	chicken prion protein
SDS	sodium dodecyl sulfate
$Hexa_4$, $chPrP_{54–77}$	chicken hexapeptide repeat prion protein fragment
$Octa_4$, $hPrP_{60–91}$	human octapeptide repeat prion protein fragment
DMSO	dimethyl sulfoxide
PrP^{Sc}	scrapie isoform of prion protein
PrP^{C}	cellular prion protein

Acknowledgements

Financial support by the National Science Centre (no. UMO-2016/23/N/ST5/01198). This work was also supported by the Italian MIUR, through the PRIN (Programmi di Ricerca di Rilevante Interesse Nazionale) Project 2015T778JW_003. The CIRMMP is also gratefully acknowledged.

Appendix A. Supplementary data

Supplementary data to this article can be found online at https://doi.org/10.1016/j.jinorgbio.2018.11.012.

References

[1] S.B. Prusiner, Science 216 (1982) 136–144.
[2] S.B. Prusiner, S.J. Dearmond, Annu. Rev. Neurosci. 17 (1994) 311–339.
[3] S.B. Prusiner, Proc. Natl. Acad. Sci. U. S. A. 95 (1998) 13363–13383.
[4] S.B. Prusiner, N. Engl. J. Med. 344 (2001) 1516–1526.
[5] D.C. Bolton, M.P. McKinley, S.B. Prusiner, Science 218 (1982) 1309–1311.
[6] S.J. Dearmond, M.P. McKinley, R.A. Barry, M.B. Braunfeld, J.R. McColloch, S.B. Prusiner, Cell 41 (1985) 221–235.
[7] M.P. McKinley, D.C. Bolton, S.B. Prusiner, Cell 35 (1983) 57–62.
[8] D.R. Brown, K.F. Qin, J.W. Herms, A. Madlung, J. Manson, R. Strome, P.E. Fraser, T. Kruck, A. vonBohlen, W. SchulzSchaeffer, A. Giese, D. Westaway, H. Kretzschmar, Nature 390 (1997) 684–687.
[9] C.S. Burns, E. Aronoff-Spencer, C.M. Dunham, P. Lario, N.I. Avdievich, W.E. Antholine, M.M. Olmstead, A. Vrielink, G.J. Gerfen, J. Peisach, W.G. Scott, G.L. Millhauser, Biochemistry 41 (2002) 3991–4001.
[10] C.S. Burns, E. Aronoff-Spencer, G. Legname, S.B. Prusiner, W.E. Antholine, G.J. Gerfen, J. Peisach, G.L. Millhauser, Biochemistry 42 (2003) 6794–6803.
[11] M. Luczkowski, H. Kozlowski, M. Stawikowski, K. Rolka, E. Gaggelli, D. Valensin, G. Valensin, J. Chem. Soc. Dalton Trans. (2002) 2269–2274.
[12] E. Gralka, D. Valensin, E. Porciatti, C. Gajda, E. Gaggelli, G. Valensin, W. Kamysz, R. Nadolny, R. Guerrini, D. Bacco, M. Remelli, H. Kozlowski, Dalton Trans. (2008) 5207–5219.
[13] F. Berti, E. Gaggelli, R. Guerrini, A. Janicka, H. Kozlowski, A. Legowska, H. Miecznikowska, C. Migliorini, R. Pogni, M. Remelli, K. Rolka, D. Valensin, G. Valensin, Chem. Eur. J. 13 (2007) 1991–2001.
[14] M. Remelli, D. Valensin, D. Bacco, E. Gralka, R. Guerrini, C. Migliorini, H. Kozlowski, New J. Chem. 33 (2009) 2300–2310.
[15] C.E. Jones, S.R. Abdelraheim, D.R. Brown, J.H. Viles, J. Biol. Chem. 279 (2004) 32018–32027.
[16] J. Shearer, P. Soh, Inorg. Chem. 46 (2007) 710–719.
[17] M.A. Wells, G.S. Jackson, S. Jones, L.L.P. Hosszu, C.J. Craven, A.R. Clarke, J. Collinge, J.P. Waltho, Biochem. J. 399 (2006) 435–444.
[18] P. Walsh, K. Simonetti, S. Sharpe, Structure 17 (2009) 417–426.
[19] V. Bonetto, T. Massignan, R. Chiesa, M. Morbin, G. Mazzoleni, L. Diomede, N. Angeretti, L. Colombo, G. Forloni, F. Tagliavini, M. Salmona, J. Biol. Chem. 277 (2002) 31327–31334.
[20] L. Calzolai, D.A. Lysek, D.R. Perez, P. Guntert, K. Wuthrich, Proc. Natl. Acad. Sci. U. S. A. 102 (2005) 651–655.
[21] P. Stanczak, M. Luczkowski, P. Juszczyk, Z. Grzonka, H. Kozlowski, Dalton Trans. (2004) 2102–2107.
[22] P. Stanczak, D. Valensin, P. Juszczyk, Z. Grzonka, C. Migliorini, E. Molteni, G. Valensin, E. Gaggelli, H. Kozlowski, Biochemistry 44 (2005) 12940–12954.
[23] E. Gralka, D. Valensin, K. Gajda, D. Bacco, L. Szyrwiel, M. Remelli, G. Valensin, W. Kamasz, W. Baranska-Rybak, H. Kozlowski, Mol. BioSyst. 5 (2009) 497–510.
[24] S.A. Thody, M.K. Mathew, J.B. Udgaonkar, Biochim. Biophys. Acta Biomembr. 1860 (2018) 1927–1935.
[25] B. Caughey, G.S. Baron, B. Chesebro, M. Jeffrey, Annu. Rev. Biochem. 78 (2009) 177–204.
[26] X.H. Wang, F. Wang, L. Arterburn, R. Wollmann, J.Y. Ma, J. Biol. Chem. 281 (2006) 13559–13565.
[27] A.T. Sabareesan, J. Singh, S. Roy, J.B. Udgaonkar, M.K. Mathew, Biophys. J. 110 (2016) 1766–1776.
[28] S.M. Butterfield, H.A. Lashuel, Angew. Chem. Int. Ed. 49 (2010) 5628–5654.
[29] J. Singh, A.T. Sabareesan, M.K. Mathew, J.B. Udgaonkar, J. Mol. Biol. 423 (2012) 217–231.
[30] H.R. Patel, A.S. Pithadia, J.R. Brender, C.A. Fierke, A. Ramamoorthy, J. Phys. Chem. Lett. 5 (2014) 1864–1870.
[31] N.S. Rösener, L. Gremer, E. Reinartz, A. König, O. Brener, H. Heise, W. Hoyer, P. Neudecker, D. Willbold, J. Biol. Chem. (2018), https://doi.org/10.1074/jbc.RA118.003116.
[32] M. Morillas, W. Swietnicki, P. Gambetti, W.K. Surewicz, J. Biol. Chem. 274 (1999) 36859–36865.
[33] A. Hecel, C. Migliorini, D. Valensin, M. Luczkowski, H. Kozlowski, Dalton Trans. 44 (2015) 13125–13132.
[34] D. Valensin, E.M. Padula, A. Hecel, M. Luczkowski, H. Kozlowski, J. Inorg. Biochem. 155 (2016) 26–35.
[35] A. Hecel, S. Draghi, D. Valensin, H. Kozlowski, Dalton Trans. 46 (2017) 7758–7769.
[36] C. Renner, S. Fiori, F. Fiorino, D. Landgraf, D. Deluca, M. Mentler, K. Grantner, F.G. Parak, H. Kretzschmar, L. Moroder, Biopolymers 73 (2004) 421–433.
[37] S.-L. Dong, S.A. Cadamuro, F. Fiorino, U. Bertsch, L. Moroder, C. Renner, Biopolymers 88 (2007) 840–847.
[38] P. Gans, A. Sabatini, A. Vacca, J. Chem. Soc. Dalton Trans. (1985) 1195–1200.
[39] G. Gran, Acta Chem. Scand. 4 (1950) 559–577.
[40] L. Alderighi, P. Gans, A. Ienco, D. Peters, A. Sabatini, A. Vacca, Coord. Chem. Rev. 184 (1999) 311–318.
[41] R.W.K. Keller, http://www.nmr.ch.
[42] T.L. Hwang, A.J. Shaka, J. Magn. Reson. 135 (1998) 280–287.
[43] D. Valensin, M. Luczkowski, F.M. Mancini, A. Legowska, E. Gaggelli, G. Valensin,

K. Rolka, H. Kozlowski, Dalton Trans. (2004) 1284–1293.
[44] W. Bal, H. Kozlowski, M. Lisowski, L. Pettit, R. Robbins, A. Safavi, J. Inorg. Biochem. 55 (1994) 41–52.
[45] H.F. Stanyon, X.J. Cong, Y. Chen, N. Shahidullah, G. Rossetti, J. Dreyer, G. Papamokos, P. Carloni, J.H. Viles, FEBS J. 281 (2014) 3945–3954.
[46] M. Klewpatinond, J.H. Viles, FEBS Lett. 581 (2007) 1430–1434.
[47] M.D. Shoulders, R.T. Raines, Annu. Rev. Biochem. 78 (2009) 929–958.
[48] A.A. Adzhubei, F. Eisenmenger, V.G. Tumanyan, M. Zinke, S. Brodzinski, N.G. Esipova, Biochem. Biophys. Res. Commun. 146 (1987) 934–938.
[49] A.A. Adzhubei, F. Eisenmenger, V.G. Tumanyan, M. Zinke, S. Brodzinski, N.G. Esipova, J. Biomol. Struct. Dyn. 5 (1987) 689–704.
[50] A.A. Adzhubei, F. Eisenmenger, V.G. Tumanyan, M. Zinke, Z. Brodsinski, N.G. Esipova, Biofizika 32 (1987) 159–161.
[51] A.A. Adzhubei, M.J.E. Sternberg, A.A. Makarov, J. Mol. Biol. 425 (2013) 2100–2132.
[52] A.A. Makarov, N.G. Esipova, Y.A. Pankov, V.M. Lobachev, B.A. Grishkovsky, Biochem. Biophys. Res. Commun. 67 (1975) 1378–1383.
[53] R. Berisio, L. Vitagliano, Curr. Protein Pept. Sci. 13 (2012) 855–865.